Heliyon 9 (2023) e14698

Contents lists available at ScienceDirect

Heliyon

journal homepage: www.cell.com/heliyon

Research article

Assessment of hemp hurd-derived biochar produced through different thermochemical processes and evaluation of its potential use as soil amendment

Marco Puglia *, Nicolò Morselli, Marluce Lumi, Giulia Santunione, Simone Pedrazzi, Giulio Allesina

BEELab (Bio Energy Efficiency Laboratory), Department of Engineering "Enzo Ferrari", University of Modena and Reggio Emilia, Via Vivarelli 10/1, 41125 Modena, Italy

ARTICLE INFO

Keywords:
Hemp hurd
Biochar
Pyrolysis
Gasification
Thermochemical process
Germinability test
Temperature
Residence time
Char properties

ABSTRACT

Biochar is a carbon-rich and porous material that finds application in different sectors and can be extremely useful in agriculture as soil improver. This paper provides a comparison between biochars produced with different slow pyrolysis processes and biochar produced in a downdraft gasifier. A blend of residual lignocellulosic biomasses (hemp hurd and fir sawdust) was pelletized and used as starting feedstock for the tests. The biochars produced were analyzed and compared. Temperature proved to be the main driver in conditioning the chemical-physical characteristics of the biochars more than residence time or the configuration of the pyrolysis process. The higher the temperature, the higher the carbon and ash content and the biochar pH and the lower the hydrogen content and the char yield. The most noticeable differences between pyrolysis and gasification biochars were the pH and the surface area (considerably higher for gasification char) and the low content of hydrogen in the gasification biochar. Two germinability tests were carried out to assess the possible application of the various biochars as soil amendment. In the first germinability test, watercress seeds were placed in direct contact with the biochar, while in the second they were placed on a blend of soil (90%v/v) and biochar (10%v/v). The biochars with the best performance were those produced at higher temperatures using a purging gas and the gasification biochar (especially mixed with soil).

1. Introduction

Biomass is considered an important and promising renewable energy source with a good prospect for power generation. Furthermore, biomass-to-power technologies can be low-cost and low-risk strategies to replace fossil fuels [1]. According to Ngamsidhiphongsa et al. [2], biomass can substitute conventional fuels because of the abundant reserves, and it is considered a carbon-neutral feedstock and can therefore reduce the emission of greenhouse gasses into the atmosphere. It is also possible to convert biomass into other products through the pyrolysis process which is a sequence of endothermic (dehydration and heating) and exothermic (volatile release and pyrolysis) reactions that degrade biomass by heating it in the absence of oxygen. During pyrolysis, biomass particles are decomposed and form char, gasses (CO, CO_2 and CH_4), condensable vapors containing organic compounds, and

* Corresponding author.
E-mail address: marco.puglia@unimore.it (M. Puglia).

https://doi.org/10.1016/j.heliyon.2023.e14698
Received 16 November 2022; Received in revised form 9 March 2023; Accepted 15 March 2023
Available online 23 March 2023

water [3]. The output of this process is biochar, bio-oil, and gaseous products [1,4]. Different types of pyrolysis lead to different products. Therefore, within certain limits, it is possible to maximize the desired product by acting on the main process parameters [3,5]. In this study, slow pyrolysis is investigated as this study focuses on biochar production, the most abundant product in slow pyrolysis processes. During slow pyrolysis, the temperature ranges from 300 to 700 °C and it is possible to obtain from 35% to 50% biochar with heating rates of 5–7 °C min^{-1} [1,3]. One of the characteristics of this type of pyrolysis is the low heating rate that allows uniform heating of the biomass particles [1]. Biochar is a carbon-rich and porous material, and its main industrial applications are relevant to the construction, plastic, paper, and textile sectors [4,6,7]. It can also be extremely valuable as soil amendment because it can increase soil organic matter and fertility, microbial activity, nutrient availability, water retention, crop yields, and good plant growth while decreasing fertilizer needs, soil and pollutant mobility [8–11]. Other agricultural applications correspond to additives for composting, silage, and feed. Furthermore, biochar has the potential for long-term carbon sequestration being recalcitrant [12]. For each of these applications, there are limit values to be respected for various parameters, such as heavy metals, organic contaminants, physical parameters, nutrients etc. [7]. The term biochar, in fact, emerged to distinguish the charred organic matter for soil applications from charcoal which is used mainly for heat or in the iron-making industry [13]. The International Biochar Initiative (IBI) provides a standardized definition of biochar as a solid material obtained from the thermochemical conversion of biomass in an oxygen-limited environment [14]. However, IBI does not prescribe the production of biochar but rather a series of characteristics that all biochars need to meet (e.g., basic utility properties such as the organic carbon content, hydrogen-organic carbon ratio, toxic thresholds for different substances etc.) [14]. The defining property of biochar is that its organic portion has a high carbon content which mainly comprises aromatic compounds characterized by rings of six atoms of carbon bound without oxygen or hydrogen. If these aromatic rings were perfectly stacked and aligned, this substance would be graphite, but the temperatures used for making biochar do not allow significant graphite formation [13]. Biochar composition depends on a variety of factors that can be related to the biomass, such as density, particle size, intrinsic biomass properties etc., or to the pyrolysis reactor operation parameters, namely temperature, residence time, heating rate, pressure etc. [13]. Biochar can also be obtained through biomass gasification that consists in the conversion of the carbonaceous material in a gaseous fuel by means of a gasifying medium (e.g. air) [8,15]. The gas produced can be used in internal combustion engines for power generation [16].

The aim of this study was to investigate the effect of different thermochemical conversion technologies and reaction conditions on the biochar properties of interest for agricultural purposes. In particular, six different pyrolysis tests and a gasification test were performed, and the biochar characteristics were evaluated to assess its potential use as soil amendment through a series of analyses (germination tests, surface area analysis, elemental and ash analysis, and pH measurements). The feedstock used for the tests was pellet composed by blending two residual biomasses, hemp hurd (50%$_{m/m}$) and fir sawdust (50%$_{m/m}$). Hemp hurd is a lignocellulosic material, fragmented in small flakes (length between 1 and 5 cm). This biomass is quite abundant and, in fact, is the main by-product of hemp fiber production [17]. Hemp hurd can be employed as filler for construction material or as fuel for combustion facilities [17]. To assess its potential use for biochar production it was pelletized with fir sawdust to improve its flowability inside the lab-scale prototypes used. In addition, the pelletization process was carried out to reduce biomass variability among different tests. The 50–50% proportion of the blend was chosen to guarantee an optimal structural integrity of the obtained pellet.

2. Materials and methods

The Cissonius PP-200 Pellet Mill [18] was used to pelletize the hemp hurd together with fir sawdust. The hemp hurd, the fir sawdust and the pellets consisting of a mixture of the two (50%$_{m/m}$ - 50%$_{m/m}$) (Fig. 1) were characterized through elemental and ash analysis.

Fig. 1. Pellets composed of hemp hurd and fir sawdust.

The ash content was evaluated measuring the mass of the residue of a sample heated at 550 °C in a Lenton ashing muffle furnace for at least 60 min, following the ISO 18122:2015 [19]. The ultimate analysis was performed through a Flash 2000 Organic Elemental Analyzer. This instrument directly measured the mass fraction of carbon, nitrogen, hydrogen, and sulfur in the sample. The reference standard used for the calibration was the BBOT – 2,5-Bis(5-*tert*-butyl-2-benzo-oxazol-2-yl). Both elemental and ash analysis were carried out on a dried sample of biomass. Knowing the elemental composition and the ash content of the dry biomass, it was possible to calculate the higher heating value (*HHV* MJ/kg) of the dry biomass through the Channiwala and Parikh [20] general correlation (Eq. (1)).

$$HHV_{bio,dry} = 0.3491C + 1.1783H + 0.1005S - 0.1034O - 0.0151N - 0.0211A \quad (1)$$

where *C*, *H*, *O*, *N*, *S* and *A* represent carbon, hydrogen, oxygen, nitrogen, sulfur, and ash contents of the biomass (expressed in mass percentage and in dry conditions). The moisture of the pellet was analyzed measuring the weight loss of a sample dried in an oven for 4 h at 105 °C (ASTM E1756-08) [21].

2.1. Pyrolysis tests

Six pyrolysis tests were carried out with four different methodologies:

- Three tests were performed through an auger pyrolyzer in retort configuration using an engine exhaust gas as hot medium. In this kind of reactor, the auger moves the biomass through an externally heated tube with no oxygen and the biomass temperature can be raised to the desired pyrolysis temperature [22].
- One test was performed using the engine exhaust gas as purging gas in a packed bed. In this test, the possibility of using the hot medium directly through the biomass was exploited.
- Two tests were performed in a cylindrical stainless steel pyrolyzer provider with electric nozzle heaters, both in retort configuration and with CO_2 as puring gas to evaluate the combination of the two methods previously described.

2.1.1. 1Auger pyrolyzer – test I, II and III

Three tests were performed using an auger pyrolyzer (Fig. 2a) with different temperatures and residence times (30 and 60 min). The auger pyrolyzer used was a stainless steel prototype made of an endless screw, a worm gear reducer with a 0.25 kW electrical motor, a vessel for the collection of the produced biochar, and a jacket around the auger wall for the passage of the hot medium (operating scheme in Fig. 2b).

Mineral wool insulation was wrapped around the steel jacket to minimize heat losses through the walls. A series of preliminary tests were performed to measure the time needed for the biomass to travel across the auger in order to assess the residence time and the mass flow of the material in the pyrolysis zone. Considering that the average time to cross the auger was 25 s, an auger length of 57.3 cm, and a length of the pyrolysis zone of 42.3 cm, the obtained time to cross the sole pyrolysis zone was estimated to be 18.5 s, (estimated biomass speed equal to 2.3 cm s^{-1}). In this condition, the residence time would be 18.5 s. To obtain a residence time of 1800 s (30 min), a reduction factor of 97.3 (97.3 ≅ 1800/18.5) need to be applied to the nominal rotation speed of the auger. A different way to obtain the same residence time without acting on the speed of rotation was by controlling the auger turn-on/off time. In particular, it was possible to obtain a residence time of 1800 s with a series of 1 s turn on time and 96.3 s (96.3 ≅ 1800/18.5–1) turn off time (or with their multiples and submultiples, such as 0.5 s and 48.2 s). With the same control logic, it was possible to implement a residence time of 3600 s (1 h). In these three pyrolysis tests, the auger motor turn on and off times were controlled through an Arduino Uno board acting

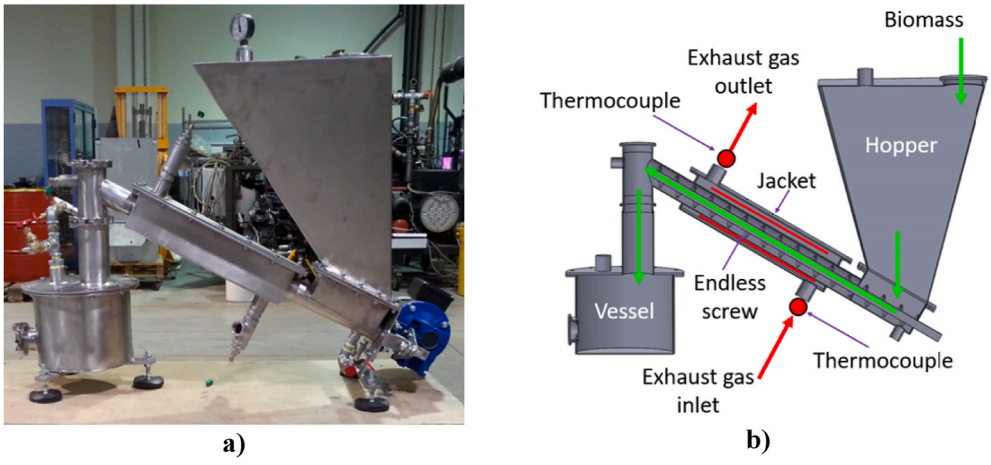

Fig. 2. (a) Auger pyrolyzer used in Tests I, II and III (b) operating scheme (adapted from Ref. [23]).

Table 1
Parameters of the tests with the auger pyrolyzer.

Test	Residence Time	Turn ON Time	Turn OFF Time	Target Temperature
I	1800 s	0.5 s	48.2 s	350 °C
II	3600 s	0.5 s	96.8 s	350 °C
III	3600 s	0.5 s	96.8 s	400 °C

on a relay switch. The heat for pyrolysis was provided by the exhaust gas of a portable internal combustion engine (Newton 4T-2700W single cylinder generator). It was possible to increase and decrease the temperature and the flow of the exhaust gas by varying the electrical load of the generator coupled to the engine through a series of lamps and a Variac voltage regulator. The exhaust pipe was connected to the jacket of the pyrolyzer.

The reference pyrolysis temperature of each test was assumed to be the average temperature which was directly measured using two K-type thermocouples, positioned at the inlet and the outlet of the jacket. The measured temperature trends during the tests inside the pyrolyzer were monitored in real time and recorded using thermocouples connected to a PicoLog Recorder [24]. The exhaust flow was calculated measuring the gasoline consumption and assuming a stoichiometric combustion. The main parameters of the three pyrolysis tests are summarized in Table 1.

It was possible to calculate the thermal power released by the exhaust gas flowing through the pyrolyzer (including thermal losses) with Eq. (2), knowing the exhaust flow and the inlet and the outlet temperatures.

$$\dot{Q}_{exh} = \dot{m}_{exh} c_{p,exh} \left(T_{exh,IN} - T_{exh,OUT}\right) = \dot{m}_{exh} c_{p,exh} \Delta T_{exh} \tag{2}$$

where c_p is the specific heat at constant pressure of the exhaust gas assumed to be the weighted average of the specific heat of the gas constituting the exhaust gas (namely Ar, CO_2, N_2 and H_2O) evaluated at the average temperature. The exhaust gas composition (mass percentage) was assumed to be 70.77% N_2, 19.76% CO_2, 8.14% H_2O, 1.29% Ar, [25]. Also knowing the biomass flow, it was possible to calculate the specific (per kg of biomass) thermal energy used with Eq. (3).

$$q_{bio} = \left(\dot{Q}_{exh}\right) / \dot{m}_{bio} \tag{3}$$

The duration of the tests was not enough to properly measure the biochar output due to the auger volume downstream the pyrolysis zone. For this reason, the estimation of the biochar output was performed considering the ash content in the biochar and in the biomass using Eq. (4), assuming a constant ash content in the solid phase:

$$\text{Biochar yield } (\%) = \frac{\text{Biomass ash content}}{\text{Biochar ash content}} \times 100 \tag{4}$$

2.1.2. *Purging gas with exhaust gas – Test IV*

This test was carried out with the aim of using the exhaust gas produced by the engine directly through the biomass-packed bed. The aim of the purging gas configuration was to increase the convective heat transfer coefficient in the reactor to improve the pyrolysis process [26]. Furthermore, purging gas can inhibit cracking or re-polymerization reactions that take place during pyrolysis [27] and affect bio-oil composition [28]. In this study, a possible effect of purging gas on the solid phase was investigated. This system consisted of two K-type thermocouples installed at the inlet and outlet of the reactor (the cylinder cartridge containing the biomass), two gate valves, and several tubes connected to each other and to the exhaust engine pipe. The pipes and tubes were wrapped with high temperature insulation (Fig. 3).

Gate valve 1 was kept closed and gate valve 2 open until the inlet temperature stabilized at about 450 °C, then 1 was opened and 2 was closed. The biomass was purged with the exhaust gas for 30 min (residence time 30 min). The reference pyrolysis temperature was assumed to be the average temperature between the temperatures measured at the inlet and at the outlet. In this test, 38 g of biomass were placed inside the reactor. Even in this case, the exhaust flow was estimated considering a gasoline stoichiometric combustion and

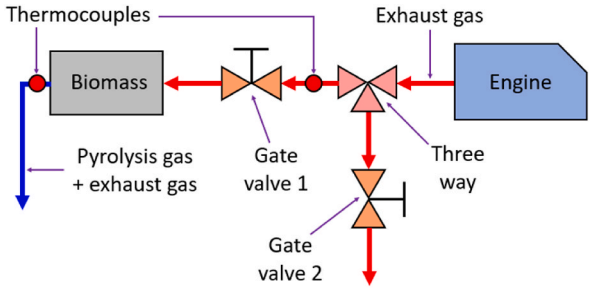

Fig. 3. Scheme of purging gas with exhaust gas setup used in Test IV.

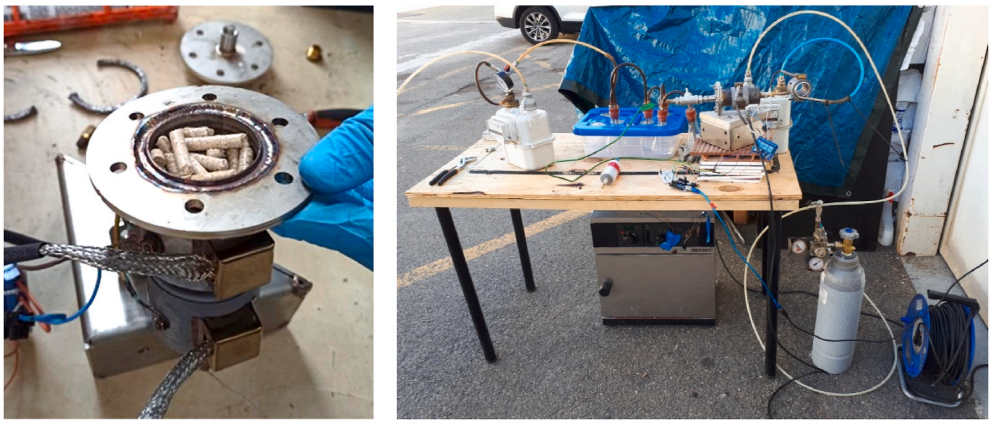

Fig. 4. Pyrolyzer with electric heaters used in Test V; reactor (a) and whole setup (b).

measuring the gasoline consumption. Being a batch test, the specific thermal energy was calculated considering the test length (residence time *t*) and the biomass placed into the reactor with Eq. (5):

$$q_{bio} = (\dot{Q}_{exh} t) / m_{bio} \tag{5}$$

2.1.3. Pyrolyzer with electric heaters – retort set-up – Test V

This test was performed using two nozzle electric heaters (230 Vac, 390 W). The heaters were wrapped around the pyrolysis reactor composed of a small cylindrical stainless steel chamber as seen in Fig. 4 (4a reactor, 4b whole pyrolysis setup).

The temperature inside the pyrolyzer was monitored by a K-type thermocouple and the turn on and turn off times of the heaters were controlled through an Arduino board and a relay switch. In this case, the target pyrolysis temperature was set between 400 and 450 °C. To avoid possible overheating of the heaters, especially during the heat up ramp, a maximum duration of the turn on time was set to 7 s, followed by a 1 s turn off time. Conversely, to avoid a possible overcooling of the pyrolysis zone, after 7 s off, there was always at a minimum 1 s on. The residence time was set to 30 min at a temperature above 400 °C inside the reactor. 97.6 g of biomass were loaded into the cylinder for the pyrolysis test. The quantity of biochar produced was directly weighed at the end of the process. Eq. (4) was used also in this test to compare the results obtained with calculation and the biochar yield directly weighed after the test. Fig. 5 illustrates the system setup for the analysis of liquid and gas produced during the pyrolysis process.

With this particular pyrolysis configuration, it was also possible to estimate the liquid and gas yield. Concerning the liquid, the produced gas was flowed through a series of impinger bottles filled with acetone, placed in a glycol ice bath, and measured after a subsequent filtration and distillation, which follows a simplified procedure deriving from the Guideline for Sampling and Analysis of Tar and Particles in Biomass Producer Gases [29,30]. Regarding the gas yield, a G4 flow meter was used to measure the gas produced during the pyrolysis process. Various gas samples were analyzed using a Pollution MicroGC GCX, calibrated for the non-condensable gasses H_2, O_2, N_2, CO, CO_2, and CH_4. Knowing the gas composition, the gas heating value was calculated as the weighted average of the heating values of the various components. The specific energy consumption of the process (including the heat losses) was measured considering the electrical power consumption of the heaters (390 W each) and recording their turn on and turn off times.

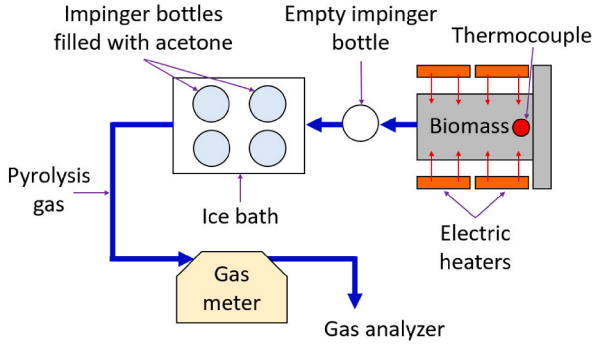

Fig. 5. Scheme of the setup with electric heaters used in Test V.

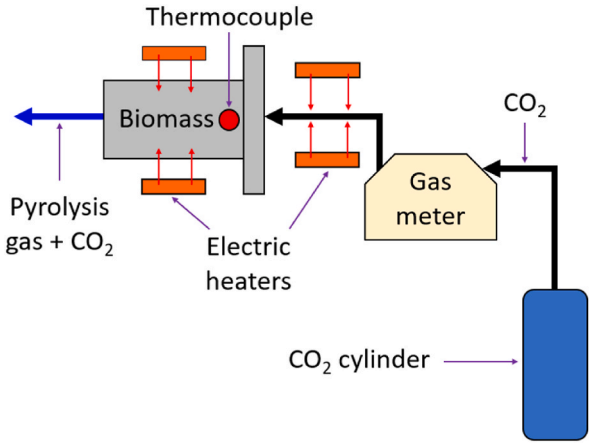

Fig. 6. Scheme of the setup with electric heaters and CO_2 as purging gas used in Test VI.

2.1.4. Pyrolyzer with electric heaters – purging gas with CO_2 setup – Test VI

This test is characterized by the flow of CO_2 through the cylindrical pyrolyzer previously described. One of the two nozzle heaters was moved from the stainless steel chamber and placed on a spiral tube to heat up the CO_2 flow to the reactor, with the other nozzle heater left wrapped around the pyrolyzer. (Fig. 6).

The Arduino board controlled the turn on and turn off times of the heaters with the same logic previously described. The residence time was set again to 30 min at a temperature above 400 °C. For this test 110 g of pellets were pyrolyzed. The CO_2 flow was set to 3.6 L per minute at standard conditions using a G4 flow meter. In this case, the gas was not analyzed because its composition moved too much from the calibration of the instrument due to the dilution of the produced gas through the CO_2 flow. The specific energy consumption of the process (including the heat losses) was measured again recording the turn on and turn off times.

2.2. Gasification test – Test VII

As a further benchmark for comparison, biochar from the gasification process was obtained through a test carried out with a laboratory-scale downdraft gasifier developed at the University of Modena and Reggio Emilia [31] (Fig. 7a picture of the system, 7b gasifier operating scheme). The aim of this test was to evaluate the possible differences between biochar obtained in an oxygen-free environment during the pyrolysis process [32] and biochar that encountered an oxidation phase during the gasification process [33].

A K-type thermocouple was placed on the gasifier grate to monitor the temperature in the reduction zone, that is, the portion of the reactor where carbon dioxide and water vapor are reduced to burnable gasses on a glowing charcoal layer [34]. Two gas samples were analyzed using the Pollution MicroGC GCX. Also in this test, the ash content of the biochar was used to estimate the biochar output using Eq. (4). It was possible to make an estimation of the biomass residence time (that can be used for the comparison with the residence times of the pyrolysis tests) by measuring the biomass flow and knowing the biomass bulk density (ρ_{bio}) and the gasifier inner volume ($V_g = 0.0016\ m^3$) with Eq. (6).

$$t = \frac{V_g \rho_{bio}}{\dot{m}_{bio}} \tag{6}$$

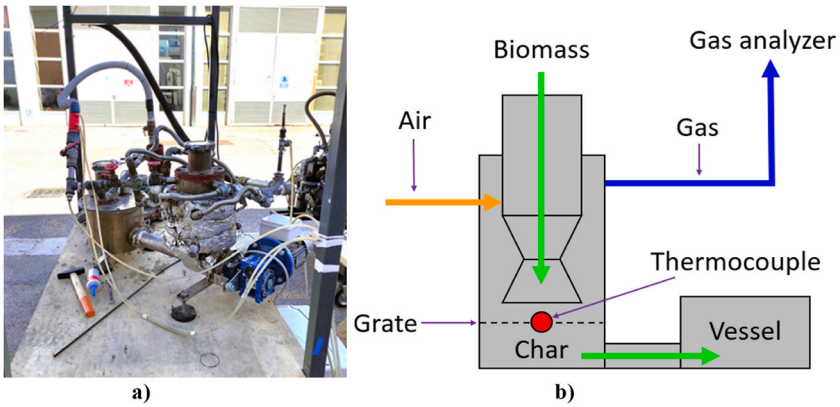

Fig. 7. Downdraft gasifier used for the gasification Test VII, picture (a) and scheme (b).

2.3. Char chemical-physical analysis

As performed for the biomass, the biochar ash content was evaluated following the standard ISO 18122:2015 and the ultimate analysis was performed through a Flash 2000 Organic Elemental Analyzer. Biochar pH was determined by adapting the methodology described by the Italian Ministerial Decree on the official methods for soil chemical analysis [35] through the potentiometric pH-Meter Crison BASIC 20 (*resolution 0.01*). 1 g of biochar was diluted in 10 ml of deionized water (1:10 biochar – water ratio), then the solution was placed on a magnetic stirrer for 30 min and filtered. Subsequently, the probe was dipped in the filtered solution for the pH measurement. Biochar is typically alkaline, and this property contributes to its liming effect and its capacity to enhance the cationic contaminant sorption of the soil. Acidic biochars are usually neglected [36].

The specific surface area of the various samples was measured through a BET (Brunauer–Emmett–Teller) analysis. The N_2 absorption–desorption was performed using a Micrometrics ChemiSorb 2750, and the calibration was carried out with a Micrometrics carbon black reference with a single point specific surface area of 21.07 ± 0.75 m^2/g. The measures were performed in triplicate for every char. For two of the seven biochar obtained, considered as the most representative of the group, a porosity analysis was performed. They were the biochar obtained with the auger pyrolyzer during test III (at higher temperature), and the biochar obtained through gasification (test VII). The first step was the determination of the bulk density and the skeletal density through a helium Pycnometer (Micrometrics AccuPyc II 1340). A 10 cm^3 nominal volume was used and the calibration was carried out with a 3.5 cm^3 reference standard. The second step was the mercury intrusion porosimetry, performed to measure the total pore volume using a Micormetrics AutoPore IV and a silica alumina reference material. The operative conditions (pressure limits 345 kPa and 228 Mpa) permitted to identify capillary pores between 0.006 and 350 μm.

Biochar performance in various applications (such as wastewater treatment) is related to its surface area and porosity, and they are important for the quantity and quality of the available active sites in the biochar. For this reason, high porosity and surface area enhance biochar cation exchange capacity, water holding capacity, and adsorption capacity [37–39].

The microstructure of different char types was investigated using Scansion Electron Microscope with Field Emission Gun (FEG) (FEI Nova NanoSEM 450). Each sample was previously metallized with a 10 nm layer of gold through a Sputter Coater (Emitech K550). The analysis was performed in high vacuum mode, using Everhart–Thornley secondary electron detector (ETD –SE). All the samples have been observed at 500×, 1000×, 2000×, 4000× and 8000× magnification in order to have a clear view of the micromorphological features and dimension of pores for each biochar type.

2.4. Germinability test

The Germination Inhibition Assay [14] is a rapid and simple analysis prescribed by the International Biochar Initiative to verify the presence of undesirable compounds in the biochar. The germinability tests were carried out in the Laboratory of Botany and *in vitro* cultures at the Life Sciences Department of the University of Modena and Reggio Emilia. Two different germination tests campaign were performed to evaluate the phytotoxicity of the biochar produced with different methodologies: in the first one, watercress seeds (*Lepidium sativum)* were placed in direct contact with biochar, while in the second one they were placed in a blend composed of 10%$_{v/v}$ of biochar and 90%$_{v/v}$ of potting soil. Watercress seeds are one of the species listed as suitable for the germination inhibition assay in the OECD guideline [40] which is the approach recommended by IBI [14] and Van Zwieten et al. [41]. The phytotoxicity of the seven biochars produced was evaluated by comparing their germinability results with the those of the control samples (without biochar). Three indices were considered to evaluate the influence of biochar on seed germination: seed germinability rate (*SG*, Eq. (7)), which considers the total and germinated seeds of each sample, the relative seed germinability rate (*RSG*, Eq. (8)), which compares the germinated seeds of the samples containing biochar with the germinated seeds of the control sample, and the relative rate of root growth (*RRG*, Eq. (9)) [42].

$$SG(\%) = \frac{n^\circ\ of\ germinated\ seeds}{n^\circ\ of\ total\ seeds} \times 100 \tag{7}$$

$$RSG(\%) = \frac{n^\circ\ of\ germinated\ seeds\ (sample)}{n^\circ\ of\ germinated\ seeds\ (control)} \times 100 \tag{8}$$

$$RRG(\%) = \frac{lenght\ of\ germinated\ seeds\ (sample)}{lenght\ of\ germinated\ seeds\ (control)} \times 100 \tag{9}$$

2.4.1. Petri dish test

In the first germinability experimental test, 20 watercress seeds were placed in a Petri dish (diameter 5.5 cm) equipped with filter paper. The same amount of each biochar sample (0.70 g) was added into the dish, in direct contact with seeds. Then, the seeds were moistened with distilled water and the dishes were sealed with parafilm, wrapped in aluminum foil, and placed at 25 °C for 36 h in the dark in an incubator (Binder ED-53). Each test was run in triplicate to obtain statistically significant results. In this germinability test type, the considered indices were SG and RG, while RRG was considered not applicable due to the absence of a proper substratum for plant growth.

Table 2
Biomass elemental and ash analysis on dry basis and moisture content.

Sample	N [%]	C [%]	H [%]	Ash [%]	HHV [MJ kg^{-1}]	Moisture [%]
Sawdust	0	49.2	6.4	0.7	20.2	/
Hemp hurd	0.3	46.4	5.9	1.2	18.4	/
Pellet	0.2	48.2	6.1	1.5	19.4	7.5

Sulfur was not detected by the instrument.

2.4.2. Blend of soil and biochar test

The second germinability experimental test was conducted using 10% biochar and 90% soil with the aim of evaluating the phytotoxicity of biochar in real conditions of application. The same amount of each biochar/soil blend type was inserted into eight seedbed incubator spaces. Two watercress seeds were placed in each seedbed space (a total of 16 seeds for each biochar/soil blend sample). 100% soil was used for the control sample. The seeds were kept moistened through the addition of distilled water. The samples were incubated for 6 days at 25 °C. In this case, all the indices were considered.

3. Results

3.1. Biomass characterization

The physical-chemical characteristics of the feedstock used and its constituents are reported in Table 2.

3.2. Test with engine exhaust gas as hot medium – Test I, II, III and IV

Fig. 8(I–IV) shows the temperature trends of the tests where the exhaust gas was used as a hot medium (test I, II, III and IV). Inlet and outlet exhaust gas temperatures are displayed together with the average temperature between the inlet and the outlet.

Table 3 reports the electric load applied to the engine in the first four tests and the corresponding gasoline consumption and calculated exhaust gas flow.

Table 4 reports the average inlet and outlet temperature during the first four tests, the average difference temperature between the inlet and the outlet, and the average value of the average temperature (between the inlet and the outlet) that was assumed as the reference pyrolysis temperature of the test.

Tests I and II have different average temperatures despite having the same engine load. This was likely due to a higher heat loss during test II. In Table 5 the specific heat at constant pressure of the various gas species considered at 357, 333 and 392 °C are reported together with the exhaust gas specific heat assumed as the weighted average.

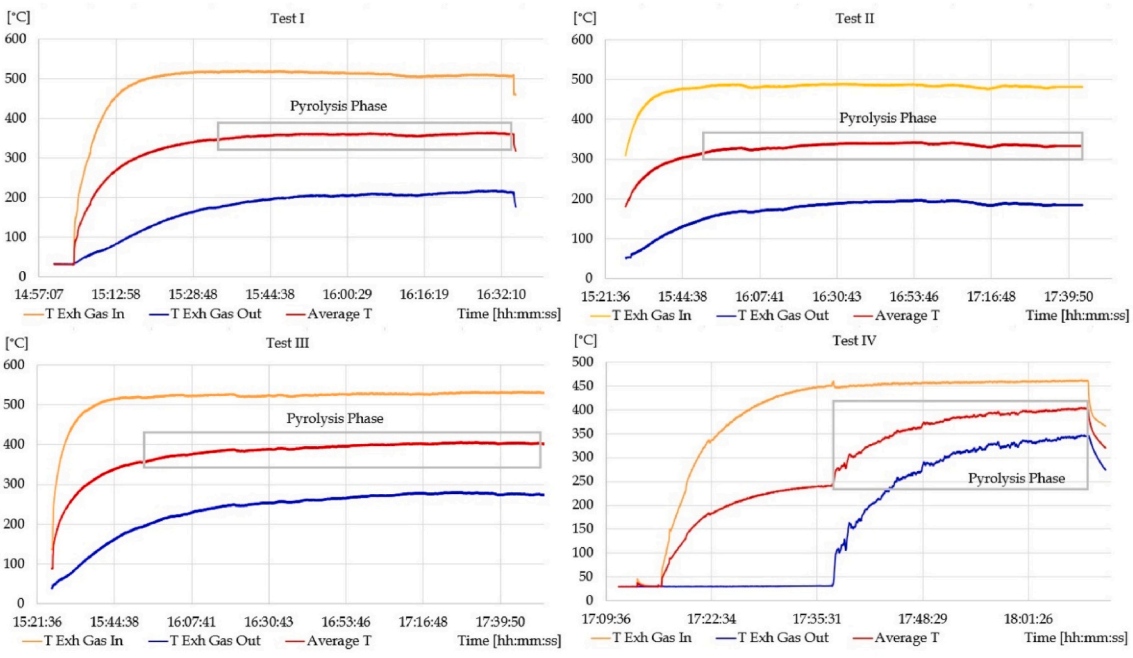

Fig. 8. Exhaust gas temperature trends, test I, II, III and IV.

Table 3
Engine electric load, gasoline consumption, and exhaust gas flow.

Test	Electric load	Gasoline consumption	Exhaust gas flow
I	690 W	0.57 kg h^{-1}	9.0 kg h^{-1}
II	690 W	0.57 kg h^{-1}	9.0 kg h^{-1}
III	888 W	0.62 kg h^{-1}	9.8 kg h^{-1}
IV	550 W	0.55 kg h^{-1}	8.7 kg h^{-1}

Table 4
Temperatures of test I, II, III and IV.

Test	Average $T_{exh,IN}$	Average $T_{exh,OUT}$	ΔT	Pyrolysis T
I	513 °C	201 °C	312 °C	357 °C
II	484 °C	182 °C	302 °C	333 °C
III	526 °C	259 °C	267 °C	393 °C
IV	456 °C	279 °C	177 °C	368 °C

Table 5
Specific heat at constant pressure of the various gas species at different temperatures.

Gas	Test I - 357 °C	Test II - 333 °C	Test III - 393 °C	Test IV - 368 °C
	c_p [J kg^{-1} $°C^{-1}$]	c_p [J kg^{-1} $°C^{-1}$]	c_p [J kg^{-1} $°C^{-1}$]	c_p [J kg^{-1} $°C^{-1}$]
H_2O	2040.4	2025.8	2062.1	2047.0
CO_2	1091.8	1080.1	1109.2	1097.1
N_2	1081.9	1076.4	1090.1	1084.4
Ar	520.6	520.6	520.6	520.6
Exh. Gas	1154.7	1147.3	1165.7	1158.1

Table 6
Biomass flow, heat power and specific energy test I, II, III and IV.

Test	Biomass flow – Biomass	$\dot{Q}$	Specific Energy
I	0.58 kg h^{-1}	903 W	5.6 MJ kg^{-1}
II	0.29 kg h^{-1}	867 W	10.8 MJ kg^{-1}
III	0.29 kg h^{-1}	849 W	10.5 MJ kg^{-1}
IV	0.038 kg	496 W	23.5 MJ kg^{-1}

The heat power released by the gas flowing through the pyrolyzer and the specific energy consumption of the various tests is summarized in Table 6.

Test I had lower specific energy. This test had the same engine load as test II, but the biomass flow was double, resulting in about twice the specific energy released during test II than was released in test I. During test II and test III, the energy released by the exhaust was roughly the same. The higher temperature and exhaust flow during test III can be attributed to a higher heat loss during test II (probably due to a slightly colder ambient temperature). Test IV, because of its configuration, had the highest release of thermal energy per kg of biomass, but it is necessary to specify that only 38 g of biomass were pyrolyzed in half an hour, respectively 13% of test I and 26% of tests II and III.

3.3. Pyrolyzer with electric heaters - retort set-up - Test V

Fig. 9 shows the temperature trend inside the reactor during the test with the electric heaters in retort setup.

The average temperature inside the reactor was 431 °C, considering the 30-min time span from the moment the temperature reached 400 °C (indicated in Fig. 9 as pyrolysis phase). The electric energy spent during the entire test amounted to 1.09 MJ (Specific Energy 11.2 MJ kg^{-1}). Tables 7 and 8 summarizes the results of test V.

It can be noticed that the percentage of solid fraction directly measured is in line with the assumed solid fraction calculated considering the ash content of the biomass and of the biochar (char yield is 30% using Eq. (4)). Table 8 reports the gas composition of the various analyzed gas samples with the corresponding heating value.

It is possible to estimate a total energy content of the produced gas of 0.19 MJ, under the assumption that the 15.5 L of gas produced during pyrolysis had an average heating value of 12.5 MJ m^{-3}. Assuming a heating value of 24.9 MJ kg^{-1} for the liquid phase [43], the heating value of the liquid product after distillation resulted in 0.39 MJ. Therefore, the thermal energy that can be obtained from burning liquid and gas was about 53% of the energy spent during the test. Considering this result, it is seemingly hard for a self-sufficient pyrolyzer to guarantee the same behavior obtained with the electric heaters during Test V. However, it is necessary to

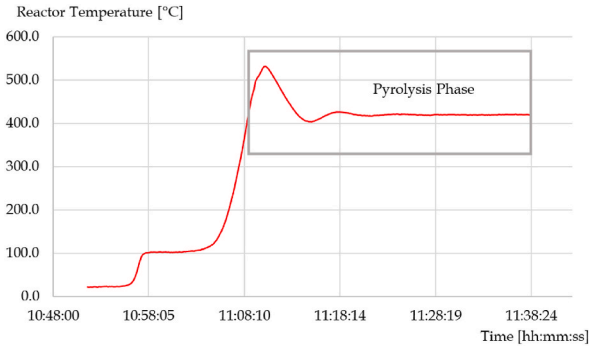

Fig. 9. Temperature trend inside the reactor, test V.

Table 7
Three phase yield during test V.

Initial biomass mass	Final solid fraction	Liquid fraction after distillation	Gas production
97.61 g (90.29 g dry)	29.46 g (33%)	15.80 g	15.5 L

Table 8
Gas composition and HHV.

Sample	H_2	CH_4	CO	CO_2	HHV
1	1.6%	9.7%	47.6%	41.1%	10.1 MJ m^{-3}
2	8.9%	17.7%	35.4%	38.0%	12.6 MJ m^{-3}
3	5.1%	24.3%	36.4%	34.2%	14.9 MJ m^{-3}

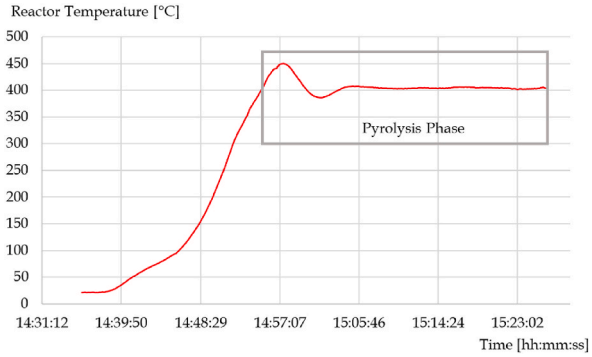

Fig. 10. Temperature trend inside the reactor, test VI.

specify that no insulation was implemented, and, hence, the heat dissipation could be greatly reduced. Furthermore, the liquid product was placed in the oven at 100 °C for 8 h to separate the water from the tars and, consequently, the most volatile fraction of the liquid was removed. For this reason, the total energy content of the liquid fraction is likely higher.

3.4. Pyrolyzer with electric heaters - purging gas with CO_2 setup – Test VI

Fig. 10 shows the temperature trend inside the reactor during the test with the electric heaters and CO_2 as purging gas.

The average temperature inside the reactor was 407 °C considering the 30-min time span from the moment the temperature reached 400 °C (indicated in Fig. 10 as pyrolysis phase). The electric energy spent during the entire test amounted to 1.56 MJ (Specific Energy 14.2 MJ kg^{-1}). In this test, the energy consumption was higher compared to the previous case without purging gas. This can be explained by the fact that a constant volume of hot gas was removed from the pyrolyzer due to the purging, while in the previous case only the gas and liquid produced during the process left the reactor.

3.5. Gasification – Test VII

Fig. 11 shows the temperature trend recorded by the thermocouple positioned on the grate of the gasification unit during the test.

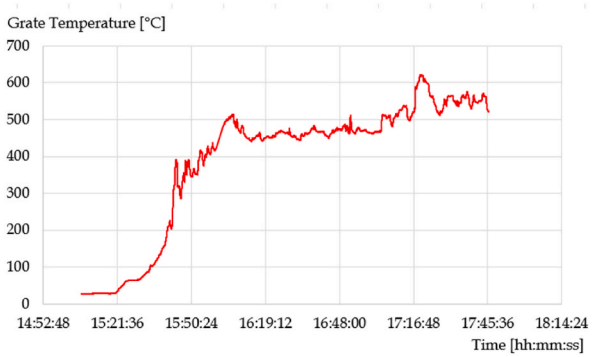

Fig. 11. Temperature trend recorded at the gasifier grate, test VII.

Table 9
Gas composition during the gasification test.

Sample	H_2 [%]	N_2 [%]	CH_4 [%]	CO [%]	CO_2 [%]	HHV [MJ m^{-3}]
1	14.2	46.8	/	27.4	9.1	5.3
2	13.6	47.1	/	26.4	11.6	5.1

The temperature remained above 450 °C once the system had reached the regime conditions. The biomass flow was 1.85 kg h^{-1}, and with Eq. (6) it is possible to calculate a residence time of 0.52 h (31 min) considering a bulk density of 600 kg m^{-3}. The gas composition of the two samples analyzed during the test is reported in Table 9.

Assuming a cold gasification efficiency (energy content of the gas divided by the energy content of biomass) of 66%, it would be possible to produce 5 kW of thermal energy. The value 66% was obtained in a previous experimental campaign when operating the same gasifier with hemp hurd as fuel [31].

3.6. Char analysis

The results of elemental, ash, specific surface area (SSA), and pH analysis carried out on different biochar samples are summarized in Table 10 together with the estimation of the biochar yield. Sulfur was not detected in any of the samples.

It is possible to see that the carbon content in the biochar resulting from high-temperature pyrolysis is higher, while they have a lower concentration of hydrogen. This result is in line with literature [44,45]. According to Gai et al. the decrease in hydrogen is due to the loss of water, tarry vapors, hydrocarbons, and gaseous H_2 [45]. While the effect of temperature on carbon is clear, the effect of residence time seems less important. Indeed, the higher carbon content was obtained with test V and VII, namely the ones with higher temperatures, while their residence time was respectively 30 and 31 min. Test II, on the other hand, had the longest residence time, but the lowest carbon content, probably due to it having the lowest average temperature of all the tests, just a few tens of degrees above the temperature of a severe torrefaction [46]. Even the specific energy seems to be less important compared to temperature. Comparing test IV with test III, and test V with test VI, it is clear that the temperature played a more important role. Regarding the content of nitrogen, the relation between temperature and nitrogen content is not straightforward. Indeed, Soka and Oyekola [44] and Hossain et al. [47] observed a first increase in nitrogen content at low pyrolysis temperatures followed by a decrease at high pyrolysis temperatures. A similar behavior can be observed in Table 10 where nitrogen content reaches a peak for test III, and then decreases for tests with higher temperatures (V and VI), and reaches the minimum for gasification biochar (VII). Additionally, the ash concentration is in line with the expectations, in particular, ash is reported to increase with pyrolysis temperature while the biochar yield decreases with

Table 10
Biochar elemental composition, ash, pH, SSA and char yield.

Sample	N	C	H	Ash	pH	SSA [g/m^2]	Char yield
I	0.3%	56.4%	5.5%	1.9%	5.23	1.17	79%*
II	0.3%	54.2%	5.6%	1.6%	5.19	2.56	94%*
III	0.4%	70.9%	4.3%	3.3%	6.59	1.90	45%*
IV	0.3%	66.9%	3.9%	3.5%	7.10	1.53	43%*
V	0.3%	80.2%	3.1%	5.0%	7.96	2.14	33%
VI	0.4%	71.9%	4.0%	4.0%	7.61	2.14	38%*
VII	0.2%	78.5%	0.9%	11.6%	9.43	11.08	13%*

*Estimated using Eq. (4).

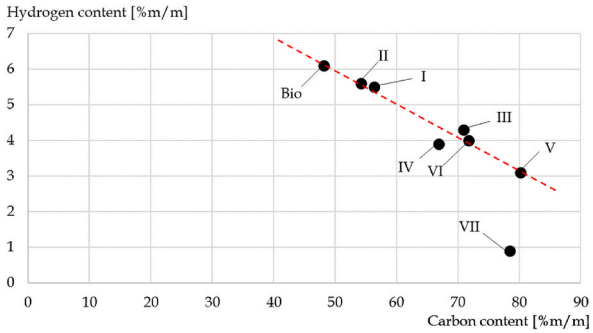

Fig. 12. Hydrogen and carbon content in the biomass and in the various biochars (I–VII).

Table 11
Bulk density, skeletal density and porosity.

Sample	Bulk density	Skeletal density	Porosity
III	0.505 g/cm^3	1.398 g/cm^3	35.28%
VII	0.447 g/cm^3	1.854 g/cm^3	62.04%

temperature [44,47]. In this work, biochar yield and ash content were considered inversely proportional to provide a rough estimation of the char yield by measuring the ash content. Concerning the biochar pH, Hossain et al. [47] obtained an acid char at low pyrolysis temperatures, an almost neutral char at 500 °C, and an alkaline biochar at high temperatures. Table 10 shows similar results for the biochar produced and examined in this work. Indeed, a high ash content is related to basic functional, while the acid functional groups related to carbon volatize with an increase of temperature [48]. The possibility of obtaining acid or alkaline biochar by varying the temperature can be intriguing for agricultural purposes because acid biochar can be used to correct alkaline soil and vice versa [47]. However, it would be important to understand if the acidity of low-temperature biochar is due to a high content of tars in the char, as the pH of bio-oil is below 3 [3,49].

As can be observed in Fig. 12, carbon and hydrogen contents of the feedstock and pyrolysis biochars remarkably fit on a linear trend. Conversely, gasification biochar shows a much sharper decrease in the hydrogen content when compared to the increase in the carbon content. This difference can be attributed to the oxidation process that takes place during gasification.

The specific surface area of the various biochar samples was in line with the specific surface area of pelletized and carbonized biomass reported in literature at similar process temperatures [37,50]. Char obtained from a pelletization process shows a lower SSA compared to its counterpart obtained from the same biomass without a pelletization process. In addition, Table 10 shows that the biochar obtained at the lowest temperature has also the lowest SSA, while the gasification char has the highest SSA (about an order of magnitude higher than the others). The most evident effect of increasing residence time without increasing the process temperature was an increase of the SSA as shown by the comparison between sample I and II; this finding is in line with the claim made by Weber and Quicker [51].

Biochar yield was lower for gasification compared to slow pyrolysis (as expected [52]), but it may be useful to point out that biochar production is not usually the primary goal of gasification, which is the provision of energy [53].

Table 11 reports bulk density, skeletal density and porosity of sample III and sample VII.

Gasification biochar (VII) presents a bulk density slightly lower compared to pyrolysis biochar (III), but on the other hand, gasification biochar has a higher skeletal density and a higher porosity. This is probably due to the higher ash content and the lower hydrogen content of the gasification biochar. Summarizing the main differences between the six samples produced through the pyrolysis process and the one produced through the gasification process they are the significantly lower hydrogen content and yield of the gasification biochar and its higher pH, SSA and porosity.

It is possible to foresee the level of conversion from the biochar color; the more the color tends to black, the higher the level of conversion [54]. Fig. 13(I–VII) shows the appearance of the various biochar samples.

The color of the obtained biochar samples was a good indicator of the level of conversion even in this case. Gasification biochar resulted the blackest, followed by the pyrolyzed ones ranked by the carbon content of the sample.

Fig. 14(I-VII) shows the microstructural analysis of the seven biochar samples obtained with SEM-FEG at 2000× magnification, using a ETD-SE detector (HV = 15.00 kV and high vacuum).

The microstructural analysis highlighted the presence of pores and deposition material on the surface of all the types of biochar. However, some differences can be noted. On sample VII (produced through gasification) the porosity is clearly visible, despite the

Fig. 13. Appearance of the biochar samples (I–VII).

deposition of other material. The pores have dimensions in the order of 10–30 μm. Additionally, the surface of samples obtained with a higher pyrolysis temperature (namely III, IV, V and VI) is also characterized by the presence of highly recognizable porous structures. The development of porous bundles follows the course of the xylem and phloem bundles of the woody component of the biomass [55].

3.7. Germinability rate test

3.7.1. Petri dishes test

Fig. 15 reports the SG while Fig. 16 reports the RSG for the different biochar types tested in direct contact with watercress seeds. The error bars represent the standard deviation of three repeated tests in case of SG, and the combination of the standard deviations of sample and control for the RSG (sum of the relative errors multiplied by the RSG value).

As shown from these two graphs, only three biochars were compatible with watercress seed germination, with values very similar to the ones obtained with the control, in particular three pyrolysis tests, IV, V, VI. The germinability rates of gasification (VII) and test (II) were almost negligible, while zero for the others. Considering the physical-chemical characteristics of the biochars, the parameter which mostly influenced the seed germination may be the pH. Both environments that are too acidic and too alkaline inhibited watercress seed germination.

3.7.2. Blend of soil and biochar test

Figs. 17 and 18 show the SG and the RSG for the biochar types tested in the soil/biochar blend. In this case, the error bars were not reported in the graphs as the test was not repeated.

In this case, all the biochars were compatible with seed germination, even biochars that completely inhibited the germination through the Petri dishes test. This is probably due to the pH correction that happened with the soil addition (soil pH equal to 7.81). The results were quite similar to one another and similar to the control values. Only test IV underperformed by a little. In this test, the RRG was also calculated, considering the seedlings' length grown due to the presence of the substrate. The RRG results are presented in Fig. 19. The error bars derive from the accuracy of the instrument used for the measurements.

As shown in the figure, two biochar types outperformed the control results, specifically VI and VII, followed by sample V whose seedlings had the same average length of the control. All other samples reached at a minimum 50% of RRG. To summarize the germinability results, the biochar that showed the best performance was test VI due to it having the best RRG in the soil/biochar blend as well as it showing very good results in all other indicators, even in the Petri dishes test, where the biochar was placed directly in contact with seeds. This may be due to an almost neutral pH. Furthermore, the CO_2 flow during the pyrolysis test could have contributed to evacuate tars or other phytotoxic substances from the biochar. Even gasification biochar (VII) shows a satisfactory germinability performance through the soil blend test. In this case the alkaline pH was corrected by the presence of soil, and the possible presence of undesired toxic components may have been prevented by the higher temperature in the reduction zone and by the gas flow that purged the char bed in the grid during the gasification test.

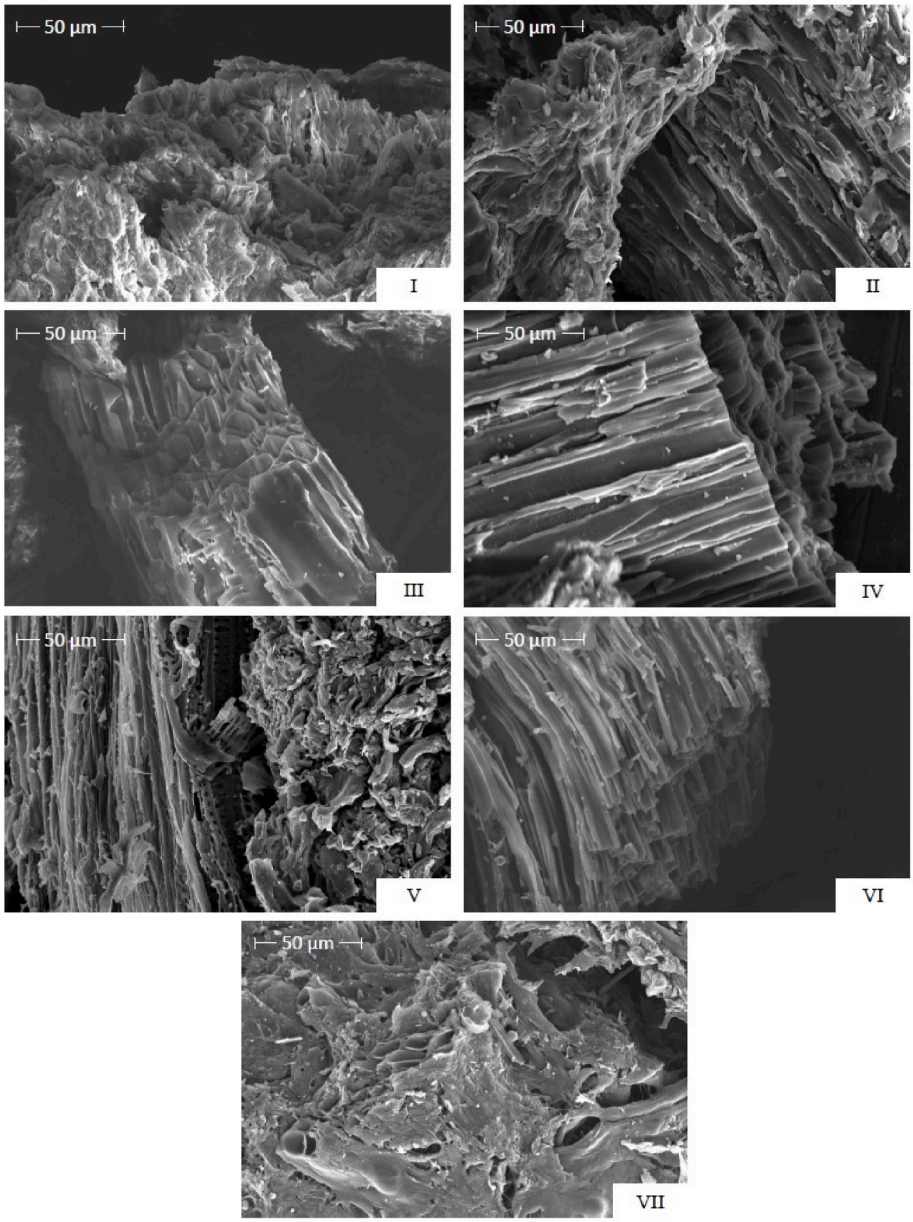

Fig. 14. Microstructures of the biochar samples (I–VII) obtained with SEM.

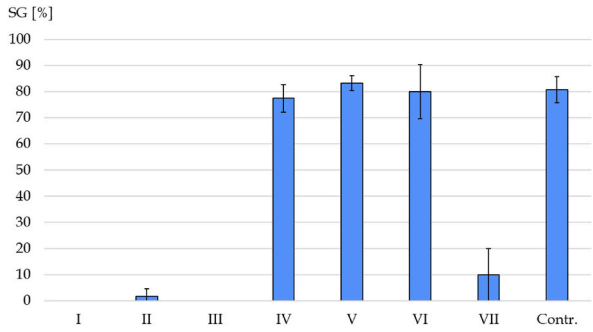

Fig. 15. Mean SG results for the various biochar types (I-VII) and control.

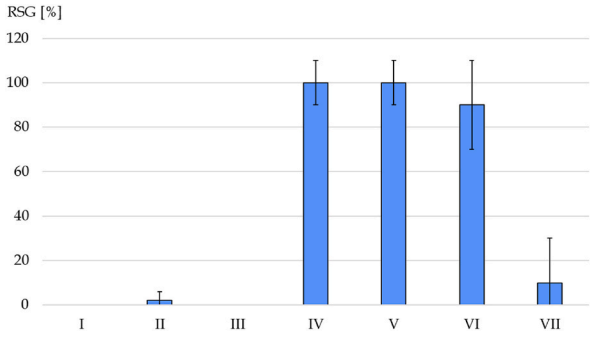

Fig. 16. Mean RSG results for the various biochar types (I-VII).

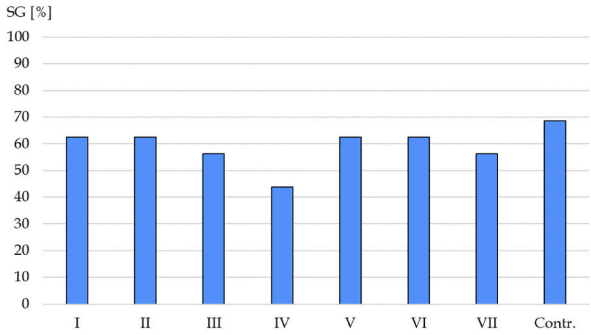

Fig. 17. SG results for the various biochar soil blends (I-VII) and control.

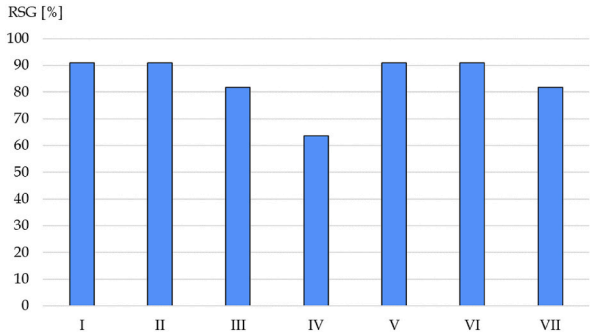

Fig. 18. RSG results for the various biochar blends (I-VII).

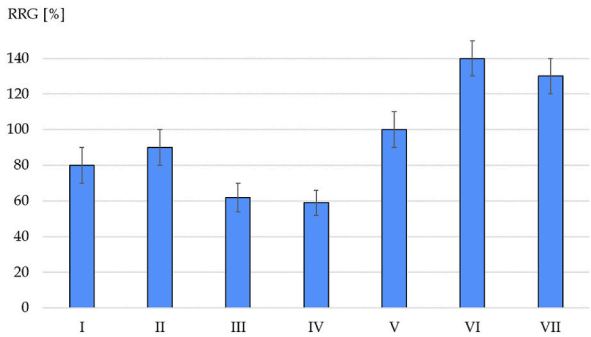

Fig. 19. RRG results for the various biochar soil blends (I-VII).

4. Conclusions

In this work, biochars produced with different methods, starting from the same feedstock, were compared to one another to assess which conditions influence the most the biochar obtained and their effect. Temperature was the most important factor that influenced the biochar physical-chemical characteristics, more than the residence time or biochar-making setup. Furthermore, the temperature of the process influences germination and plant growth, affecting the pH of the biochar. The concurrence of high temperature and gas purging through the biochar during the process gave better results on average, in terms of high carbon content and high germinability rate. This could be due to a more homogeneous heat exchange mechanism and to the evacuation of tars located in the biochar. The amount of energy used for the various processes seemed to only partially affect the biochar product. Increasing the residence time can be less effective than increasing the temperature of the process (at the same power provided). For this reason, a process that is able to reach high temperatures and with the presence of purging gas could be the best solution, unless an acid biochar is the product goal, or a lower-temperature heat source is available at extremely advantageous conditions. Concerning the main differences between pyrolysis and gasification, biochar obtained through gasification showed a much higher pH, porosity and specific surface area, and a much lower hydrogen–carbon ratio and yield. The next steps of this work will be to assess the crystal structure of biochars obtained with different thermochemical processes by means of an XRD analysis and to compare their effect on plant growth through their application to soil in pot tests.

Author contribution statement

Marco Puglia, Nicolò Morselli: Conceived and designed the experiments; Performed the experiments; Analyzed and interpreted the data; Contributed reagents, materials, analysis tools or data; Wrote the paper.

Marluce Lumi, Giulia Santunione: Performed the experiments; Analyzed and interpreted the data; Contributed reagents, materials, analysis tools or data; Wrote the paper.

Simone Pedrazzi, Giulio Allesina: Conceived and designed the experiments; Analyzed and interpreted the data; Contributed reagents, materials, analysis tools or data; Wrote the paper.

Funding statement

This research did not receive any specific grant from funding agencies in the public, commercial, or not-for-profit sectors.

Data availability statement

Data will be made available on request.

Declaration of interest's statement

The authors declare that they have no known competing financial interests or personal relationships that could have appeared to influence the work reported in this paper.

References

[1] L. Chen, C. Wen, W. Wang, T. Liu, E. Liu, H. Liu, Z. Li, Combustion behaviour of biochars thermally pretreated via torrefaction, slow pyrolysis, or hydrothermal carbonisation and cofired with pulverised coal, Renew. Energy 161 (2020) 867–877.

[2] N. Ngamsidhiphongsa, P. Ponpesh, A. Shotipruk, A. Arpornwichanop, Analysis of the Imbert downdraft gasifier using a species-transport CFD model including tar-cracking reactions, Energy Convers. Manag. 213 (2020), 112808.

[3] P. Basu, Biomass Gasification and Pyrolysis: Practical Design and Theory, Elsevier Inc., 2010, ISBN 978-0-12-374988-8.

[4] J.J. Manyà, Pyrolysis for biochar purposes: a review to establish current knowledge gaps and research needs, ES T (Environ. Sci. Technol.) 46 (2012) 7939–7954.

[5] M. Garcia-Perez, T. Lewis, C.E. Kruger, Methods for Producing Biochar and Advanced Biofuels in Washington State. Part 1: Literature Review of Pyrolysis Reactors, First Project Report, Department of Biological Systems Engineering and the Center for Sustaining Agriculture and Natural Resources, Washington State University, Pullman, WA, 2010, p. 137.

[6] A. Korus, G. Ravenni, K. Loska, I. Korus, A. Samson, A. Szlęk, The importance of inherent inorganics and the surface area of wood char for its gasification reactivity and catalytic activity towards toluene conversion, Renew. Energy 173 (2021) 479–497, https://doi.org/10.1016/j.renene.2021.03.130.

[7] EBC (2012–2022) 'European Biochar Certificate—Guidelines for a Sustainable Production of Biochar'. European Biochar Foundation (EBC), Arbaz, Switzerland. Version 10.1 from 10 January 2022. Available online: http://european-biochar.org (accessed on 19 June 2022).

[8] L. Li, Z. Yao, S. You, C.H. Wang, C. Chong, X. Wang, Optimal design of negative emission hybrid renewable energy systems with biochar production, Appl. Energy 243 (2019) 233–249, https://doi.org/10.1016/j.apenergy.2019.03.183.

[9] X.X. Guo, H.T. Liu, J. Zhang, The role of biochar in organic waste composting and soil improvement: a review, Waste Manag. 102 (2020) 884–899, https://doi.org/10.1016/j.wasman.2019.12.003.

[10] S. Jones, R.P. Bardos, P.S. Kidd, M. Mench, de F. Leij, T. Hutchings, A. Cundy, C. Joyce, G. Soja, W. Friesl-Hanl, R. Herzig, P. Menger, Biochar and compost amendments enhance copper immobilisation and support plant growth in contaminated soils, J. Environ. Manag. 171 (2016) 101–112, https://doi.org/10.1016/j.jenvman.2016.01.024.

[11] S. Jeffery, F.G.A. Verheijen, M. van der Velde, A.C. Bastos, A quantitative review of the effects of biochar application to soils on crop productivity using meta-analysis, Agric. Ecosyst. Environ. 144 (1) (2011) 175–187, https://doi.org/10.1016/j.agee.2011.08.015.

[12] C.J. Atkinson, J.D. Fitzgerald, N.A. Hipps, Potential mechanisms for achieving agricultural benefits from biochar application to temperate soils: a review, Plant Soil 337 (2010) 1–18, https://doi.org/10.1007/s11104-010-0464-5.
[13] J. Lehmann, S. Joseph, Biochar for environment management: science and technology, Ch 1-2, 1-16, Earthscan, 2009. ISBN: 978-1-84407-658-1.
[14] IBI, Standardized product definition and product testing guidelines for biochar that is used in soil, international biochar initiative, Available online: http://www.biochar-international.org/characterizationstandard, 2015 (accessed on 28 June 2022).
[15] S. Mishra, R. Kumar Upadhyay, Review on biomass gasification: gasifiers, gasifying mediums, and operational parameters, Materials Science for Energy Technologies 4 (2021) 329–340, https://doi.org/10.1016/j.mset.2021.08.009.
[16] A. Shah, R. Srinivasan, S.D.F. To, E.P. Columbus, Performance and emissions of a spark-ignited engine driven generator on biomass based syngas, Bioresour. Technol. 101 (2010) 4656–4661.
[17] C. Ingrao, A. Lo Giudice, J. Bacenetti, C. Tricase, G. Dotelli, M. Fiala, V. Siracusa, C. Mbohwa, Energy and environmental assessment of industrial hemp for building applications: a review, Renew. Sustain. Energy Rev. 51 (2015) 29–42, https://doi.org/10.1016/j.rser.2015.06.002.
[18] Cissonius, Available online: https://pellet-mill.de/PP200-Pellet-Mill, 2022 (accessed on 17 August 2022).
[19] ISO 18122:2015 Solid Biofuels-Determination of Ash Content.
[20] S.A. Channiwala, P.P. Parikh, A unified correlation for estimating HHV of solid, liquid and gaseous fuels, Fuel 81 (8) (2002) 1051–1063, https://doi.org/10.1016/S0016-2361(01)00131-4e.
[21] ASTM E1756-08(2020) Standard Test Method for Determination of Total Solids in Biomass.
[22] M.I. Jahirul, M.G. Rasul, A.A. Chowdhury, N. Ashwath, Biofuels production through biomass pyrolysis —a technological review, Energies 5 (12) (2012) 4952–5001, https://doi.org/10.3390/en5124952.
[23] M. Puglia, Design and Tests of a Table-Top Facility for the Thermochemical Valorization of Agricultural Residues through Pyrolysis and Gasification, Ph.D. Thesis, University of Modena and Reggio Emilia, 2021.
[24] Pico technology, Available online: https://www.picotech.com/library/data-loggers/picolog-6-data-logger-software, 2022 (accessed on 17 August 2022).
[25] M. Puglia, N. Morselli, S. Pedrazzi, P. Tartarini, G. Allesina, A. Muscio, Specific and cumulative exhaust gas emissions in micro-scale generators fueled by syngas from biomass gasification, Sustainability 13 (6) (2021) 3312, https://doi.org/10.3390/su13063312.
[26] L. Ding, X. Shi, J. Zhang, Y. Wu, C. Wang, J. Gao, X. Lan, Modeling on the pyrolysis of particles of low-rank coal and CaO mixture, J. Anal. Appl. Pyrol. 156 (2021), 105169, https://doi.org/10.1016/j.jaap.2021.105169.
[27] J. Akhtar, N.S. Amin, A review on operating parameters for optimum liquid oil yield in biomass pyrolysis, Renew. Sustain. Energy Rev. 16 (7) (2012) 5101–5109, https://doi.org/10.1016/j.rser.2012.05.033.
[28] P. Kim, S. Weaver, N. Labbé, Effect of sweeping gas flow rates on temperature-controlled multistage condensation of pyrolysis vapors in an auger intermediate pyrolysis system, J. Anal. Appl. Pyrol. 118 (2016) 325–334, https://doi.org/10.1016/j.jaap.2016.02.017.
[29] J.P.A. Neeft, H.A.M. Knoef, U. Zielke, K. Sjoestroem, P. Hasler, P.A. Simell, M.A. Dorrington, L. Thomas, N. Abatzoglou, S. Deutch, et al., Guideline for sampling and analysis of tar and particles in biomass producer Gases, version 3.3, Energy Project ERK6-CT1999-20002 (Tar Protocol). Available online: http://www.tarweb.net/results/pdf/guideline-3.3-v2.pdf, 2002 (accessed on 14 July 2022).
[30] Y. Chen, Y. Wang, L. Pezzola, R. Mussi, L. Bromberg, J. Heywood, E. Kasseris, A novel low-cost tar removal technology for small-scale biomass gasification to power, Biomass Bioenergy 149 (2021), 106085, https://doi.org/10.1016/j.biombioe.2021.106085. ISSN 0961-9534.
[31] S. Pedrazzi, N. Morselli, M. Puglia, F. Ottani, M. Parenti, Equilibrium modeling of hemp hurd gasification, in: 28th European Biomass Conference and Exhibition, 2020, pp. 450–454, https://doi.org/10.5071/28thEUBCE2020-2CV.3.22.
[32] FAO, Food and Agriculture Organization of the United Nations, Industrial Charcoal Making, FAO Forestry Paper 63, Mechanical Wood Products Branch Forest Industries Division FAO Forestry Department, 1985, ISBN 92-5-102307-7.
[33] FAO, Food and Agriculture Organization of the United Nations, Wood Gas as Engine Fuel, FAO Forestry Paper 72, Mechanical Wood Products Branch Forest Industries Division FAO Forestry Department, 1986, ISBN 92-5-102436-7.
[34] SERI, Solar Energy Research Institute, U.S. Department of Energy, Generator Gas the Swedish Experience from 1939-1945, 3rd Edition with Index, ISBN 1-890607-01-0.
[35] MIPAF, Ministero delle politiche agricole e forestali, Approvazione dei "Metodi ufficiali di analisi chimica del suolo", Decreto Ministeriale 13/09/1999, Supplemento ordinario alla "Gazzetta Ufficiale" n.248 del 21 ottobre 1999 - Serie generale.
[36] F. Qi, Z. Dong, D. Lamb, R. Naidu, N.S. Bolan, Y. Sik Ok, C. Liu, N. Khan, M.A.H. Johir, K.T. Semple, Effects of acidic and neutral biochars on properties and cadmium retention of soils, Chemosphere 180 (2017) 564–573, https://doi.org/10.1016/j.chemosphere.2017.04.014.
[37] L. Leng, Q. Xiong, L. Yang, H. Li, Y. Zhou, W. Zhang, S. Jiang, H. Li, H. Huang, An overview on engineering the surface area and porosity of biochar, Sci. Total Environ. 763 (2021), 144204, https://doi.org/10.1016/j.scitotenv.2020.144204.
[38] Wang S., Zhang H., Wang J., Hou H., Du C., Ma P. C., Kadier A., Application of Biochar for Wastewater Treatment, In: Thapar Kapoor, R., Treichel, H., Shah, M. P. (eds) Biochar and its Application in Bioremediation. Springer, Singapore. https://doi.org/10.1007/978-981-16-4059-9_4.
[39] A. Promraksa, N. Rakmak, Biochar production from palm oil mill residues and application of the biochar to adsorb carbon dioxide, Heliyon 6 (5) (2020), E04019, https://doi.org/10.1016/j.heliyon.2020.e04019.
[40] OECD Organisation for Economic Co-operation and Development, Terrestrial plants, growth test no. 208, in: Guideline for Testing of Chemicals, 1984. https://www.oecd.org/chemicalsafety/risk-assessment/1948285.pdf (Accessed on 2 August 2022).
[41] L. Van Zwieten, S. Kimber, S. Morris, K.Y. Chan, A. Downie, J. Rust, S. Joseph, A. Cowie, Effects of biochar from slow pyrolysis of papermill waste on agronomic performance and soil fertility, Plant Soil 327 (2010) 235–246, https://doi.org/10.1007/s11104-009-0050-x.
[42] S. Pedrazzi, G. Santunione, M. Mustone, G. Cannazza, C. Citti, E. Francia, G. Allesina, Techno-economic study of a small scale gasifier applied to an indoor hemp farm: from energy savings to biochar effects on productivity, Energy Convers. Manag. 228 (2021), 113645.
[43] K. Raveendran, Anuradda Ganesh, Heating value of biomass and biomass pyrolysis products, Fuel 75 (15) (1996) 1715–1720, https://doi.org/10.1016/S0016-2361(96)00158-5.
[44] O. Soka, O. Oyekola, A feasibility assessment of the production of char using the slow pyrolysis process, Heliyon 6 (7) (2020), e04346, https://doi.org/10.1016/j.heliyon.2020.e0434.
[45] Gai X., Wang H., Liu J., Zhai L., Liu S., Ren T., Liu H., Effects of feedstock and pyrolysis temperature on biochar adsorption of ammonium and nitrate, nitrate. PLoS One 9(12): e113888. doi:10.1371/journal.pone.0113888.
[46] W.H. Chen, J. Peng, X.T. Bi, A state-of-the-art review of biomass torrefaction, densification and applications, Renew. Sustain. Energy Rev. 44 (2015) 847–866, https://doi.org/10.1016/j.rser.2014.12.039.
[47] M.K. Hossain, V. Strezov, K.Y. Chan, A. Ziolkowski, P.F. Nelson, Influence of pyrolysis temperature on production and nutrient properties of wastewater sludge biochar, J. Environ. Manag. 92 (1) (2011) 223–228, https://doi.org/10.1016/j.jenvman.2010.09.008.
[48] R. Janu, V. Mrlik, D. Ribitsch, J. Hofman, P. Sedláček, L. Bielská, G. Soja, Biochar surface functional groups as affected by biomass feedstock, biochar composition and pyrolysis temperature, Carbon Resources Conversion 4 (2021) 36–46, https://doi.org/10.1016/j.crcon.2021.01.003.
[49] W.H. Chen, S.H. Liu, T.T. Juang, C.M. Tsai, Y.Q. Zhuang, Characterization of solid and liquid products from bamboo torrefaction, Appl. Energy 160 (2015) 829–835, https://doi.org/10.1016/j.apenergy.2015.03.022.
[50] K. Januszewicz, P. Kazimierski, M. Klein, D. Kardas, J. Łuczak, Activated carbon produced by pyrolysis ofWaste wood and straw for PotentialWastewater adsorption, Materials 13 (9) (2020) 2047, https://doi.org/10.3390/ma13092047.
[51] K. Weber, P. Quicker, Properties of biochar, Fuel 217 (2018) 240–261, https://doi.org/10.1016/j.fuel.2017.12.054.
[52] S. You, Y. Sik Ok, S.S. Chen, D.C.W. Tsang, E.E. Kwon, J. Lee, C.H. Wang, A critical review on sustainable biochar system through gasification: energy and environmental applications, Bioresour. Technol. 246 (2017) 242–253, https://doi.org/10.1016/j.biortech.2017.06.177.

[53] Y. Neubauer, 6 - biomass gasification, editor(s): lasse rosendahl, in: Woodhead Publishing Series in Energy, Biomass Combustion Science, Technology and Engineering, Woodhead Publishing, 2013, ISBN 9780857091314, pp. 106–129, https://doi.org/10.1533/9780857097439.2.106.
[54] A.A. Boateng, C.A. Mullen, Fast pyrolysis of biomass thermally pretreated by torrefaction, J. Anal. Appl. Pyrol. 100 (2013) 95–102, https://doi.org/10.1016/j.jaap.2012.12.002.
[55] A. Rawal, S.D. Joseph, J.M. Hook, C.H. Chia, P.R. Munroe, S. Donne, Y. Lin, D. Phelan, D.R.G. Mitchell, B. Pace, J. Horvat, J.B.W. Webber, Mineral–biochar composites: molecular structure and porosity, Environ. Sci. Technol. 50 (14) (2016) 7706–7714, https://doi.org/10.1021/acs.est.6b00685.